 doi:10.20944/preprints202203.0080.v1

# *Residual stresses in VT6 (Ti-6Al-4V) alloy after shot peening evaluated using X-ray Diffraction, Laser Speckle Interferometry and Ga-ion FIB-DIC micro-ring-core milling*

Somov P.A.[1], Statnik E.S.[1,*], Kan Yu.[1], Pisarev V.S.[2], Eleonsky S.I.[2], Ozherelkov D.Yu.[3], and Salimon A.I.[1,3]

[1] HSM lab, Skoltech, Moscow 121205, Russia

[2] Central Aero-Hydrodynamics Institute named after Prof. N.E. Zhukovsky (TsAGI), Zhukovsky 140180, Russia

[3] National University of Science and Technology "MISiS", Moscow 119991, Russia

[*] Correspondence: eugene.statnik@skoltech.ru

**Abstract:** Shot peening has become a well-established technique for the introduction of beneficial compressive Residual Stresses (RS) into the near-surface layers of metallic materials for the purpose of preventing or suppressing fatigue crack nucleation and growth. Ti-alloys are widely used to fabricate compressor blades of aeroengines. Titanium blades that may be susceptible to different modes of damage under cyclic loading (high cycle fatigue, fretting fatigue) are often subjected to shot peening to extend their safe operating time. The control and monitoring of residual stresses in titanium blades is of great importance to assure the safety of aeroengines. The techniques for residual stress evaluation include mechanical methods (material removal) as well as physical methods such as X-ray diffraction. Perhaps the most common and practically accessible form of the latter is the $sin^2\psi$ method. Conventional laboratory X-ray diffractometers typically probe samples to the depths up to ~20 µm that correspond to 1x...5x the average grain size for typical metals and alloys. The limitations of the $sin^2\psi$ method have been identified and reviewed in the literature, motivating the use of other semi-destructive approaches to evaluate the residual stresses in deeper layers and at more sharply defined locations. In the present report we present a case study of the comparison between non-destructive and semi-destructive evaluation techniques, namely the $sin^2\psi$ X-ray diffraction method against the mechanical and FIB-DIC ring-core drilling applied to the samples of VT6 (Russian designation of Ti-6Al-4V) titanium alloy after shot peening with 1 mm steel balls. Mechanical drilling of circular holes of ~2 mm diameter with laser speckle interferometry monitoring of strains gives a rough spatial resolution of a few millimeters, while the Korsunsky FIB-DIC method of Ga-ion beam micro-ring core milling within FIB-SEM with Digital Image Correlation (DIC) deformation analysis delivers spatial resolution down to a few micrometers. Good agreement has been found between the X-ray and FIB-DIC estimates of RS variation profiles as a function of depth in shot peened titanium alloy samples. Some

 doi:10.20944/preprints202203.0080.v1

advances in the FIB-DIC method are presented and discussed in terms of the acceleration of data acquisition and interpretation.

**Keywords:** residual stress, VT6 (Ti-6Al-4V), shot peening, X-ray diffraction $sin^2\psi$, speckle interferometry, Ga-ion FIB-DIC

## 1 Introduction

Shot peening is a cold processing technique that can significantly extend the working lifespan of components undergoing intense loads due to a favorable compressive layer of Residual Stresses (RS) and modifying the mechanical properties by hardening, removing corrosion or mechanical surface defects like burrs or stripes after metalworking, etc.

Many various manufacturing processes used in aerospace, aviation, automotive mostly create tensile stresses on the component surfaces. Typically, these methods include milling, drilling, turning, welding, heat treatment, and their combinations that provide tensile stress on the surface, thereby creating an ideal environment for cracks initiation or stress corrosion formation, inevitably reducing the lifespan of the parts [1].

The key feature of the shot peening technique is protecting the material against corrosion-mechanical and fatigue damage that frequently forms on the metal surface. Each shot plastically deforms the material during the processing and creates a compressive layer of the residual stresses on the surface that prevents cracks initiation and propagation and significantly improves the material's strength, reliability, and durability [2,3].

The steel or cast iron shots with a particle size of 0.5-2.0 mm are usually used in the shot peening. The optimal particle speed during the contact with the surface part is 50-70 m/s, the angle of shots incidence is 75-90$^o$, processing time usually does not exceed 2-3 minutes, during which shots treat and penetrate surface layers at a depth of 0.2-0.4 mm. After that time, 'saturation' effect is coming and process does not cause noticeable changes in the quality and condition of the surface layers [4].

There are several methods that can measure and control the shot peening process, i.e., obtain profile and distributions of induced residual stresses. For instance, X-Ray Diffraction (XRD) is the most common non-destructive technique that can measure the absolute stress values and does not require a non-stress calibrated specimen. However, it has a main limitation connected with the significant penetration depth of the X-ray beam that affects the scale of the collected information. Alternative methods like hole drilling are destructive and also measure macroscopic residual stresses [5]. However, it is well-known that residual stress

Preprints (www.preprints.org) | NOT PEER-REVIEWED | Posted: 4 March 2022 doi:10.20944/preprints202203.0080.v1

is an additive characteristic that separates the following three types of RS at the different scale levels, namely, $\epsilon = \epsilon_I + \epsilon_{II} + \epsilon_{III}$, where $\epsilon_I$ covers macroscopic RS, $\epsilon_{II}$and $\epsilon_{III}$ are responsible for local microscopic (several grains) and intragranular RS, respectively [6,7].

In order to separate and extract RS from the microscopic scale level, the Focused Ion Beam - Digital Image Correlation (FIB-DIC) ring-core milling technique has been developed by Korsunsky *et al*. [8]. The Korsunsky method is based on step-wise material removal and obtaining relief strains by digital image correlation of Scanning Electron Microscope (SEM) images.

In this article, we measured residual stresses in VT6 (Ti-6Al-4V) alloy after shot peening using X-ray diffraction, laser speckle interferometry, and Ga-ion FIB-DIC micro-ring-core milling at the different scale levels. Moreover, we characterized the microstructure and measured the hardness of the non-treated and shot-peened surfaces by Electron Backscatter Diffraction (EBSD) and nanoindentation techniques.

## 2 Materials and methods

### *2.1 Sample preparations*

The 90x7.5x3 $mm^3$ plates of VT6 alloy (produced by VSMPO-AVISMA Inc., Verkhnya Salda, Russia) were cut using an Electrical Discharge Machining (EDM) Mitsubishi MV-1200R (Abamet LLC, Moscow, Russia) from a drawn bar. The surfaces 90x7.5 $mm^2$ were additionally mechanically polished to reach roughness $R_a = 3.2\mu m$ and $R_z = 25.2\mu m$. Polished samples were annealed at 630 °C for 2 hours in vacuum to relax residual stresses introduced during polishing.

The steel balls (used in bearing) with diameter of 1.5 mm were accelerated with an ultrasonic agitating device to shot peen the surface of plates with colliding velocity of about 10 m/s. The construction of shot peening chamber where plates were fixed at the roof provided the treatment in the middle zone approximately 50 mm long. The appearance of titanium plate and the position of shot peened window are given (blue frame) in Figure 1. One of shot peened plates was EDM sectioned into smaller parts (red lines) for various further analyses:

- ***Transition zone part*** included both shot peened and non-treated areas. The techniques of nanoindentation and FIB-DIC evaluation of RS were applied to probe the surface characteristics in terms of mechanical response and in-plane residual stresses;
- ***Three 7.5x5x3 $mm^3$ parts*** were carefully prepared for EBSD studies of microstructure and FIB-DIC evaluation of RS in deep layers under shot peened surface. The faces 7.5x3 $mm^2$ (***Face I***), 5x3 $mm^2$

Preprints (www.preprints.org) | NOT PEER-REVIEWED | Posted: 4 March 2022 doi:10.20944/preprints202203.0080.v1

(***Face II***) and 7.5x5 mm$^2$ (***Face III***) were mechanically polished with a set of sandpapers, diamond pastes (1-3 µm) and colloidal silica, and then finished with ion gun Leica EM RES 102 (Leica Microsystems, Wetzlar, Germany) under the next regime: voltage 6 kV, current 2.6 mA, gun tilt 3°, milling time 1 hour;

- ***X-ray 1*** (shot peened surface) and ***X-ray 2*** (non-treated surface) parts were used to investigate RS in surface layer with help of X-ray ($sin^2\psi$) method.

We discuss below the assumptions and limitations of $sin^2\psi$ method in respect of finding of FIB-DIC.

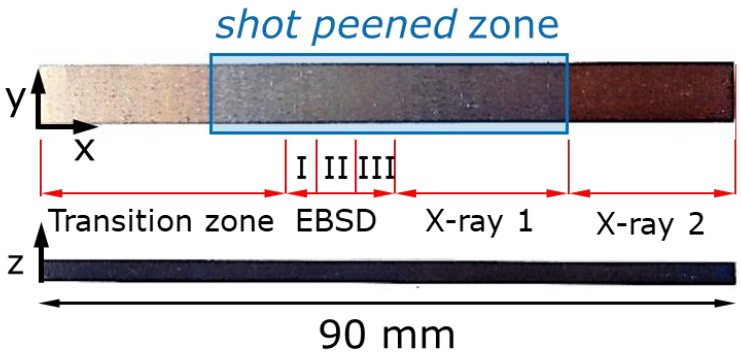


**Figure 1.** Initial specimen with the indicated coordinate system, dimensions, and regions of interest along which it was cut

*2.2 X-ray Diffraction ($sin^2\psi$) method*

A diffractometer XRD Bruker D8 Advance (Bruker AXS Inc., Madison, Wisconsin, USA) with Cu $K_\alpha$ wavelength of 0.154 nm dedicated for the study of powder samples was used to carry out $sin^2\psi$ measurements. Due to the lack of option for side-tilting, a special sample holder (a single degree of freedom goniometer) was fabricated to allow sample inclination of 0, 10, 20, 30 and 40 degrees, whilst the X-ray source and detector were continuously scanned over the $2\theta$ angle range 110-127 degrees. The tilting sample holder shown in Figure 2 was designed and 3D-printed. By rotating the holder, it was possible to apply $\varphi$-tilting to determine residual stresses along the sample long axis, and $\omega$-tilting for the transverse direction.

Acquired spectra were processed with the following data treatment pipeline: spectra fitting, background subtraction and centre peak positions for the calculation of $d_{HKL}$. In this case, residual stress can be determined from the slope of the $d$ versus $sin^2X$ graph, where $d$ is measured lattice spacing and $X$ is the tilt angle.

Preprints (www.preprints.org) | NOT PEER-REVIEWED | Posted: 4 March 2022 doi:10.20944/preprints202203.0080.v1

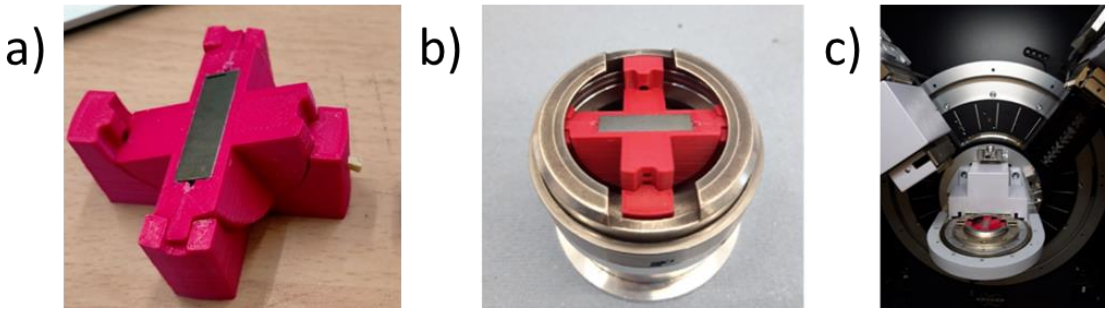


**Figure 2.** The details of X-ray diffraction ($sin^2\psi$) technique realization: a) goniometer-like setup, b) setup embedded into diffractometer grip, and c) setup with grip into diffractometer

*2.3 Mechanical hole drilling and laser speckle-interferometry*

The hole-drilling method is a destructive technique for the experimental evaluation of residual stress in materials [9]. The removal of a certain amount of material with help of hole drilling (blind or through) causes the release of residual stress energy and local deformation - diameter increment or decrement. The detection of deformation response to drilling is a task requiring adequate sensitivity and accuracy since the strains to be measured are of about few thousandth and, therefore, few micrometer displacements must be detected for few millimeter big hole diameters. Drilling with a diameter 1.9 mm drill was applied. The distance between blind 2.5 mm deep holes varied in the range of 10…15 mm.

The details of experimental setup design for electronic speckle-pattern interferometry (ESPI) applied was published previously [10,11]. Optical detecting system uses normal illumination (diode laser with wavelength of 532 nm) with respect to plane object surface and two symmetrical detectors (digital photo cameras) to record interferograms. Phase shift in respect to the surface interferogram before drilling forms specific patters - fringes, the number of which is easily re-calculated to the diameter increment (with the respective sign) by means of multiplication by the factor $\lambda/2\,sin\theta$ , where $\lambda$ is incident illumination light wavelength, and $\theta$ is the angle between incident and reflected beam.

*2.4 Nanoindentation technique*

A NanoScan-4D system (FSBI TISNCM, Troitsk, Russia) was used to probe mechanical performance of VT6 sample at the surface using Oliver-Pharr method [12]. Diamond Berkovich indenter was used at the regime: linear increment of force to reach 3 N in 10 s, 0.6 s holding, and unloading with the same force rate. Young's modulus and hardness were calculated with fused silica calibration and then processed to introduce work-of-indentation correction recommended for ductile materials [13].

Preprints (www.preprints.org) | NOT PEER-REVIEWED | Posted: 4 March 2022 doi:10.20944/preprints202203.0080.v1

*2.5 FIB-SEM studies: Microscopy, EBSD and FIB-DIC ring-core drilling*

A dual Ga-FIB FEG-SEM S9000 Solaris microscope (Tescan Orsay Holding, Brno, Czech Republic) was used for SE and BSE visualization of surface topography and EBSD (detector by Oxford Instruments NanoAnalysis and Asylum Research, High Wycombe, UK) characterization of structure - phase composition, grain size, shape and orientation (texture) distribution with help of AZtec software (integrated software from Oxford Instruments supplied with the detector).

Areas for EBSD analysis were 200 and 400 $\mu m^2$ with efficient pixel size of 1 $\mu m^2$ for data collection at acceleration voltage of 20 kV and beam current 10 nA.

The Korsunsky focused ion beam ring-core drilling method (FIB-DIC) is a destructive method for the evaluation of residual stresses at micrometer scale [8]. Residual stresses of Type I, II and III may be under some assumptions prescribed to the entities of different dimensional scale, namely, to an assembly of many grains, a single grain and intragrain domains respectively [7]. Averaged over sufficiently large volume in a single grain, residual stresses of Type III return the estimation for Type II. In the same way, the average value of residual stresses of Type II taken from a sufficient number of single grains is equal to residual stresses of Type I. These are the engineering scale residual stresses that directly correspond to the results of FE modeling based on continuous mechanics of solids. Thus, the representability and robustness of residual stress evaluation with FIB-DIC ring-core method depend on the ratio between core diameter and grain size - when a number or many of grains are present inside given core of ring drill, the value of strain, appeared as a result of core unloading and respective residual strain release, correspond to Type I residual stress in a certain locality. EBSD characterization of grain structure becomes a necessary preliminary step for correct selection of geometrical parameters of FIB ring-core drilling. Particular voltage-current of ion milling were empirically found and optimized in accordance with general recommendations given in [14] for this method to be the following: high voltage 30 kV, current 10 nA, tilt stage 55°, 10 µm inner diameter and 15 µm outer diameter of a ring, milling depth 1 µm/step, dataset of 12 images.

*2.6 DIC processing*

DIC (*iStress* software [15]) of image subsets is applied to detect the strains of a $10^{-4}…10^{-2}$ for the core diameters of 1…10 µm. High resolution imaging at relevant magnification is required to reveal sufficient density of contrasting features inside core for robust DIC. Sample preparation for EBSD analysis includes ion finishing that forms a specific surface topography enriched with noticeable grain boundaries and triple

Preprints (www.preprints.org) | NOT PEER-REVIEWED | Posted: 4 March 2022 doi:10.20944/preprints202203.0080.v1

boundary joints - these surface features were customized for contrasting and purposeful selection of localities for FIB ring-core drilling.

## 3 Results and Discussion

### *3.1 Structure characteristics*

Grain maps collected using EBSD scanning and contrasted with Euler colors for shot peened part are assembled in pseudo-cubic and represented in Figure 3(a) in the cross-sections corresponding to the axes *x*, *y* and *z* designated in Figure 1. No difference in general appearance of grain patterns is detectable with naked eye. Relatively small (5…10 μm) and equiaxial grain of α-Ti phase are found in all cross-sections, although pole charts clearly show strong texture with preferential orientation of (0001) planes in the samples. Grains of β-Ti phase (the volume fraction is less than 3 %) are much smaller (0.5 …1 μm) and mainly located along grain boundaries and in few triple grain joints. No peculiarities were recognized in subsurface layers of shot peened areas where the influence of severe plastic deformation caused by repetitive impacts might be anticipated.

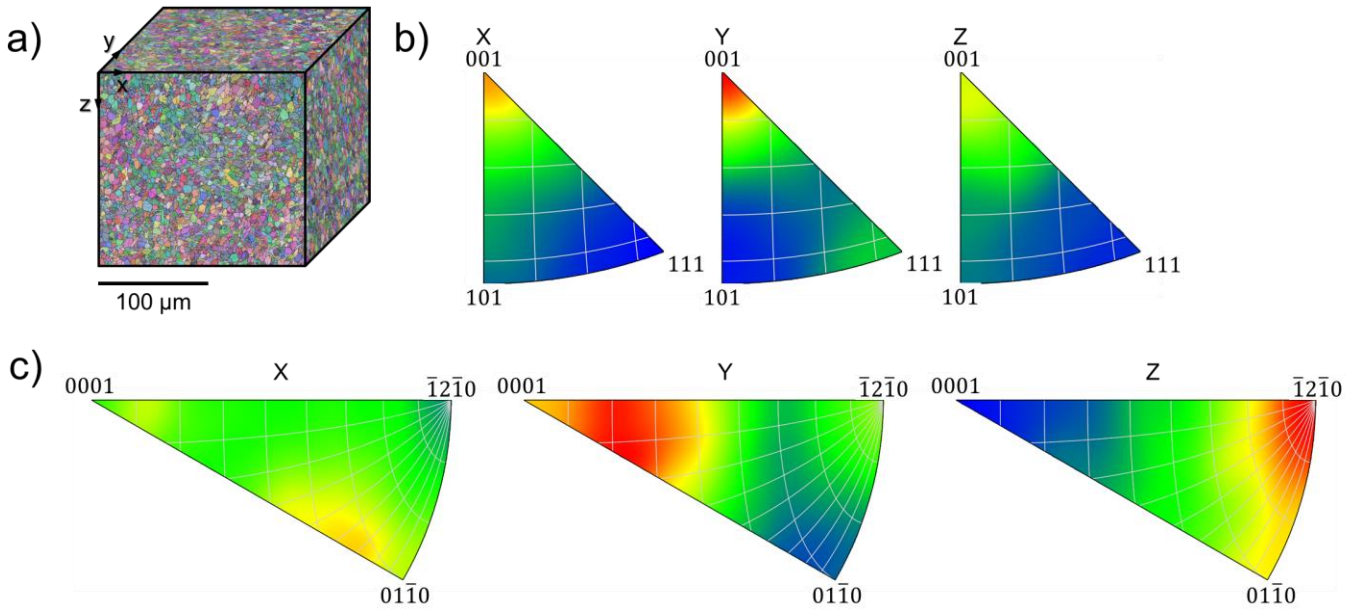


**Figure 3.** Structure characteristics of a shot peened VT6 samples: a) pseudo-cubic of Euler color maps and IPF color maps for b) β-Ti and c) α-Ti, respectively

### *3.2 Macroscopic mechanical hole drilling*

Preprints (www.preprints.org) | NOT PEER-REVIEWED | Posted: 4 March 2022 doi:10.20944/preprints202203.0080.v1

Three drilled holes are shown in Figure 4 and they characterize non-treated (1 and 2) and shop peened (3) areas.

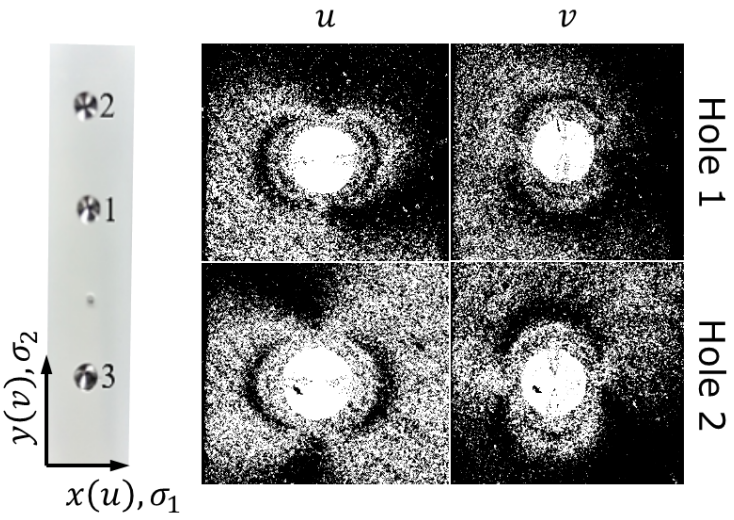


**Figure 4.** Appearance of drilled holes and interferograms for holes 1 and 2

Relatively weak and almost isotropic residual tensile stresses were detected in the non-treated areas: 5 fringes along $u$ axis mean $\sigma_1$ = +83 MPa (Young's modulus 115 GPa, Poisson's coefficient 0.35) and 4,5 fringes along $v$ correspond to $\sigma_2$ = +79 MPa. Surprisingly, no fringes could be imaged for hole 3 and other holes drilled in the shot peened area, what we relate to either instrumental issues (specific surface relief in the shot peened area, perhaps, makes fringes too noisy) or to the fact of averaging of tensile and compressive residual stresses when significant thickness comparable with the thickness of plate is analyzed. This directly points on the necessity to apply techniques relevant to smaller thickness in terms of spatial resolution especially when relatively thin layers are affected. From the surface appearance images taken in the ***Transition zone*** in the vicinity of about 5 µm deep indents (Figure 5) one can conclude that system of scratches remained after mechanical polishing is slightly modified towards less regular relief with the signs of deformation and smashing of asperities. The tracks of scratches are visible down to the bottom of indents (about 5 µm). Nevertheless, scratches are clearly recognizable suggesting that severe plastic deformation did not propagated much deeper than 5 µm, while general thickness of shot peening affected zone is believed to be bigger by a factor of 3…5. The resolution of residual stresses in depth, therefore, might have to be comparable with this value, i.e. to be about 20 µm, what fairly corresponds to the estimation based on the average grain size - few grain diameters also returns the scale parameter of about 20 µm.

Preprints (www.preprints.org) | NOT PEER-REVIEWED | Posted: 4 March 2022 doi:10.20944/preprints202203.0080.v1

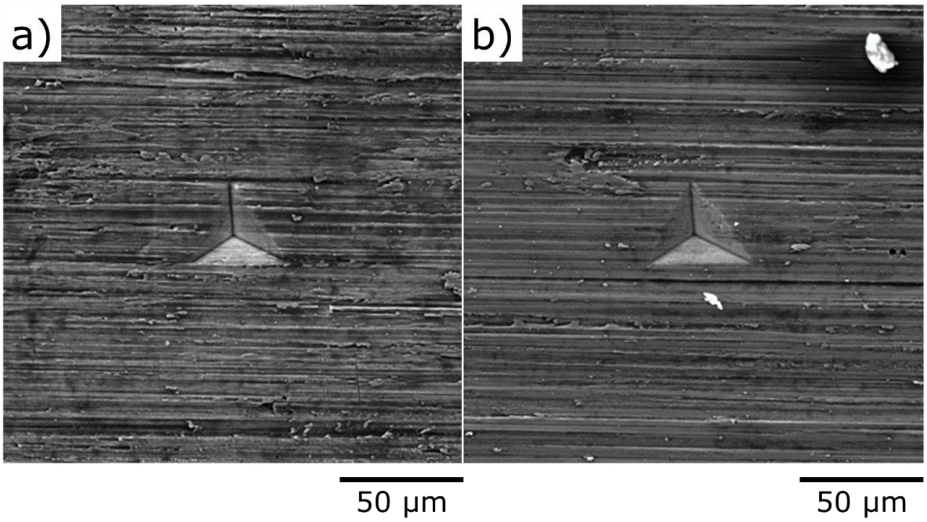


**Figure 5.** Appearance of VT6 sample surface a) shot peened; b) non-treated

*3.3 Hardness measurements*

Probing of mechanical response at the surface shows some hardening of shot peened materials against non-treated one, namely, 2.79±0.14 GPa against 2.48±0.17 GPa as seen from Figure 6.

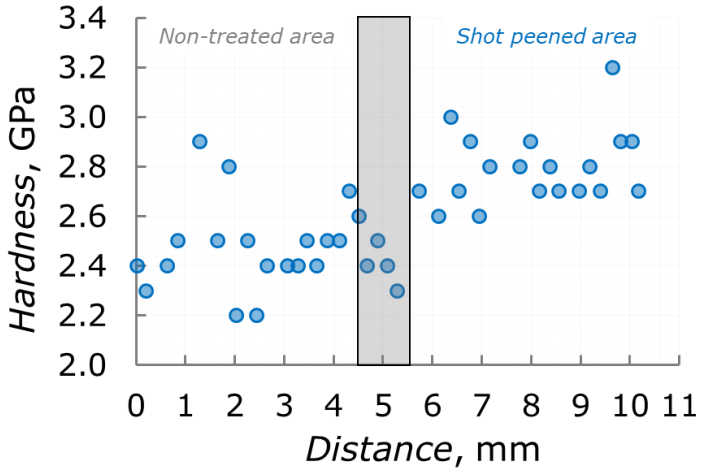


**Figure 6.** Hardness of VT6 alloy in the ***Transition zone*** sample

Some work hardening due to the severe plastic deformation is supposed to be the main reason of this difference in hardness. As we discussed above it does not seem that layer of plastic deformation caused by shot peening may propagate to depth for more than first tens of micrometers.

*3.4 X-ray diffraction evaluation of residual stresses*

Preprints (www.preprints.org) | NOT PEER-REVIEWED | Posted: 4 March 2022 doi:10.20944/preprints202203.0080.v1

Typical X-ray spectra acquired for $\psi$ = 0, 10, 20, 30 and 40 degrees as well as $d$ against $sin^2\psi$ linearization plot are demonstrated in Figure 7. It is worth to note that gradual shift of peak with the increase of $\psi$ is easily noticeable with naked eye suggesting good sensitivity of the method even when noisy spectra are analyzed like that in Figure 7a. Strong dependence of signal-to-noise ratio on the sample orientation is obviously related with the texture that was discovered by EBSD.

The data on peak shift and estimates of residual stresses for two $(hkl)$ crystallographic directions in α-Ti and one $(hkl)$ in β-Ti phases are accumulated in Table 1. Compressive residual stresses along both *x* and *y* sample's axis as strong as -1000 MPa have been detected at the both sides of sample where the shot peening treatment was applied - shot peening gives good uniformity and reproducibility of treatment. Compressive residual stresses along (212) direction seems to be at least for 30 % stronger than along (105) (close to (001)) direction also suggesting predominant concentration of eigenstrains within non-basal planes of hexagonal lattice of α-Ti. No reliable conclusions can be made on residual stresses due to the wide spread (values differing by more than a factor of 3) of measured values along different sample axes and at different sample sides.

The data on residual stresses in non-treated area are not (or much less) statistically reliable, however, relatively small tensile stresses appear to be present. These might be inherited from previous sample treatments which affected the material, including forging/rolling, annealing, cutting and mechanical polishing. The presence of small tensile residual stresses is detected by the mechanical hole drilling method, suggesting their preservation both at the surface and in the deep subsurface layers.

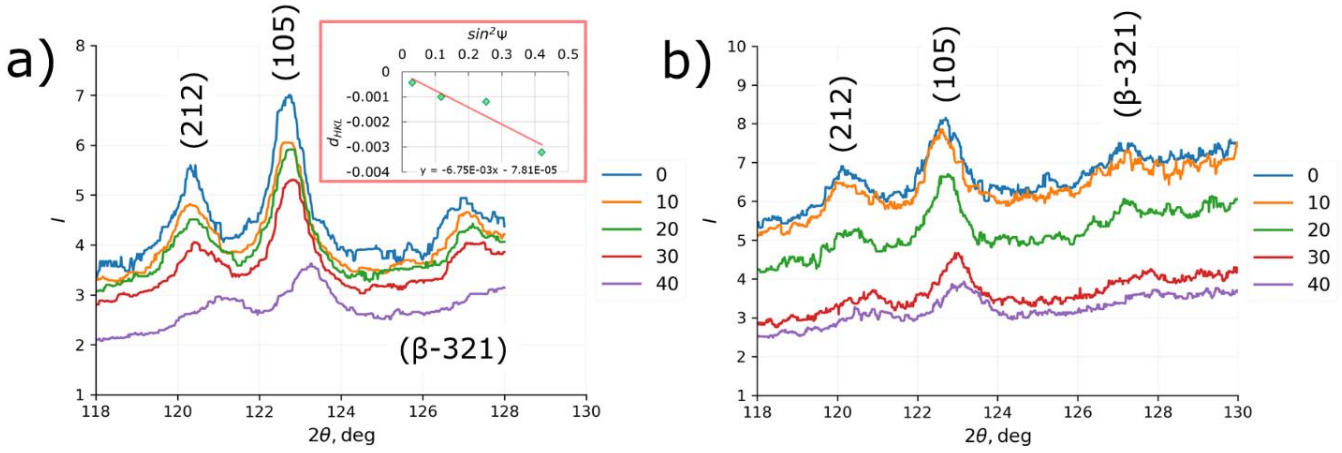


**Figure 7.** X-ray diffraction spectra collected for $\psi$ = 0, 10, 20, 30 and 40 degree from ***X-ray 1*** specimen aligned along sample's a) $x$ axis and b) $y$ axis. Inset is a plot of $d_{HKL}$ vs $sin^2\psi$ linearization plot.

Preprints (www.preprints.org) | NOT PEER-REVIEWED | Posted: 4 March 2022 doi:10.20944/preprints202203.0080.v1

**Table 1.** Residual stresses in ***X-ray 1*** (shot peening) and ***X-ray 2*** (non-treated) specimens of VT6. The estimations of residual stress for correlation coefficient below 0.85 (absolute value) are given in Italic typeset

| Sample | $(hkl)$ | Peak position, 2θ degree | | | | | Residual stress, MPa | Correlation coefficient |
|---|---|---|---|---|---|---|---|---|
| | | $\psi = 0^o$ | $\psi = 10^o$ | $\psi = 20^o$ | $\psi = 30^o$ | $\psi = 40^o$ | | |
| **X-ray 1** (along sample's $x$ axis) | (212) | 120.2 | 120.2 | 120.3 | 120.7 | 120.8 | -1330.1 | 0.97 |
| | (105) | 122.6 | 122.6 | 122.7 | 122.9 | 123.1 | -964.6 | 0.98 |
| | (β-321) | 127.1 | 127.1 | 127.3 | 127.4 | 127.6 | -907.8 | 0.99 |
| **X-ray 1** *back side* (along sample's $x$ axis) | (212) | 120.3 | 120.3 | 120.3 | 120.6 | 120.9 | -1318.9 | 0.97 |
| | (105) | 122.6 | 122.6 | 122.6 | 122.8 | 123.1 | -1011.3 | 0.95 |
| | (β-321) | 127.3 | 127.0 | 127.2 | 127.2 | 127.6 | -522.6 | 0.73 |
| **X-ray 1** (along sample's $y$ axis) | (212) | 120.4 | 120.3 | 120.5 | 120.4 | 121.1 | -1273.1 | 0.86 |
| | (105) | 122.7 | 122.7 | 122.8 | 122.8 | 123.2 | -931.9 | 0.89 |
| | (β-321) | 126.7 | 127.1 | 127.2 | 127.2 | 127.8 | -1794.1 | 0.91 |
| **X-ray 1** *back side* (along sample's $y$ axis) | (212) | 120.3 | 120.3 | 120.3 | 120.6 | 120.1 | -1478.4 | 0.98 |
| | (105) | 122.6 | 122.6 | 122.7 | 122.9 | 123.2 | -1002.4 | 0.96 |
| | (β-321) | 127.1 | 127.1 | 127.1 | 127.5 | 127.7 | -1042.8 | 0.97 |
| **X-ray 2** (along sample's $x$ axis) | (212) | 121.0 | 120.9 | 120.8 | 120.9 | 120.9 | 118.9 | 0.34 |
| | (105) | 123.1 | 123.1 | 123.1 | 123.1 | 123.1 | -34.3 | 0.40 |
| | (β-321) | 127.7 | 127.6 | 127.7 | 127.6 | 127.7 | 32.3 | 0.06 |
| **X-ray 2** (along sample's $y$ axis) | (212) | 120.7 | 120.7 | 120.7 | 120.7 | 120.8 | 237.3 | 0.86 |
| | (105) | 122.9 | 122.9 | 122.9 | 122.9 | 122.9 | 291.0 | 0.87 |
| | (β-321) | 127.5 | 127.6 | 127.5 | 127.5 | 127.6 | 97.3 | 0.21 |

Residual stresses in shot peened area show weak dependence on the crystallographic orientation $(hkl)$ of grains assuming that residual stress is relatively isotropic in the surface layer regardless strong texture detected by EDSD. It is likely that severe plastic deformation activates many slip systems in α-Ti crystalline lattice including non-basal planes - that averages stress state formed in the surface layer.

The $sin^2\psi$ method owes its popularity to the advantage of its convenient implementation within laboratory diffractometers. However, it is also subject to a number of significant shortcomings that have been critically discussed previously [16].

Four assumptions underlying conventional $sin^2\psi$ method are as follows:

Preprints (www.preprints.org) | NOT PEER-REVIEWED | Posted: 4 March 2022 doi:10.20944/preprints202203.0080.v1

A1. The penetration of the X-ray beam is so shallow that the material interrogated can be thought to be in the state of plane stress.

A2. The grain ensemble contributing to the diffraction peak is representative of the state of deformation in the sample as a whole.

A3. Despite the polycrystalline nature of the sample, it can be represented correctly by a homogeneous elastic continuum.

A4. Even in the presence of plastic deformation which causes residual stresses, correct values of the diffraction elastic constants (DEC's) can be identified, and Hooke's law can be applied to relate stresses and strains.

Whilst it is important to emphasize that all these assumptions are approximate and do not hold in practice, for the present purposes it is worth focusing attention on Postulate A3 that deals with data interpretation based on continuum homogeneous elasticity. In fact, polycrystalline samples consist of multiple grains of different orientations with different elastic and plastic properties. The strains in this grain ensemble are different from a uniform continuum. Furthermore, sample tilting leads to data collection from different grain groups, which may lead to significant deviations that affect the results.

The conclusion is drawn at this stage that the outcomes of the $sin^2\psi$ method are likely to be subject to significant aberrations that may reach 20-30 % systematic or random error, and need to be supported with measurements using other independent methods to improve reliability of interpretation.

### *3.5 Residual stresses at microscopic level – FIB-DIC evaluation results*

*Shot peened surface.* Figure 8a is a superposition of ***Transition zone*** specimen SEM image and designations of locations where FIB core-ring drilling was used to probe residual stresses at the surface of shot peened and non-treated areas. Locations $(01\bar{1}0)$ are generally aligned along $x$ axis and in the middle of sample. Locations 11 and 12 are as close as 100 µm to the edges – 11 is close to EDM cut, while 12 corresponds to the longest edge of sample in the shot peened area. Figure 8b depicts the estimates of residual stresses which were present at the sample surface before drilling. The series of indents (hardness measurements) is also visible in Figure 8a.

Preprints (www.preprints.org) | NOT PEER-REVIEWED | Posted: 4 March 2022 doi:10.20944/preprints202203.0080.v1

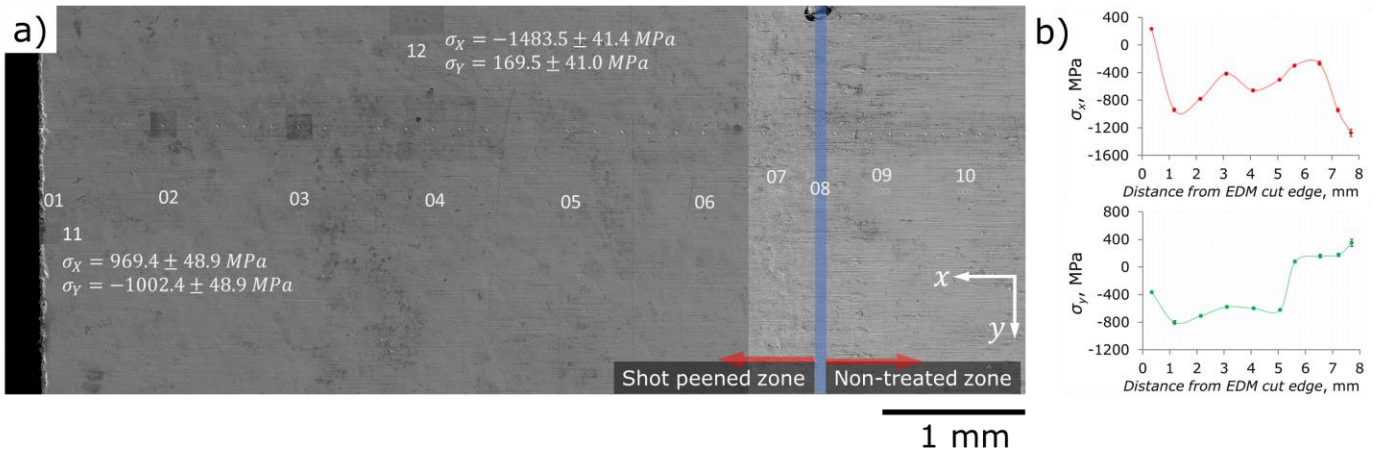


**Figure 8.** FIB-DIC evaluation of RS at the surface in the ***Transition zone*** specimen: a) location of FIB-DIC probing; b) profile of RS along $x$ and $y$ axes

A number of observations can be done from a fast glance:

- Locations 02…06 show approximately equal values of compressive residual stresses $\sigma_x$ and $\sigma_y$ in both principal directions in the range of -800…-400 MPa. This is in good agreement with the estimations of X-ray measurements.
- Locations 07…10 as well as 11 and 12 where some peculiarities of sample geometry or treatment are undoubtedly present - edges or boundary of shot peened and non-treated areas - reveal strong asymmetry of residual stresses. This asymmetry means both different signs of stresses and enormous absolute difference in the values of stresses - for at least 1600 MPa. Location 01 also shows different signs of $\sigma_x$ and $\sigma_y$, but absolute difference is somewhat smaller - of about 600 MPa.
- At the edges tensile stresses exist.
- The boundary between shot peened and non-treated areas from residual stresses point view occurs much broader than that which can be recognized from the difference in surface appearance. Considering the locations 07…10 as belonging to the boundary area the width of this area may be assessed as 2 mm (2 shot peening balls diameters).

Emergence of tensile residual stresses at these peculiarities is stated of great importance – the promotion of nucleation and growth of fatigue cracks becomes possible in some directions even for shot peened parts, which are theoretically protected against cracking phenomena due the introduction of compressive stresses. EDM cutting is considered as the least invasive macroscopic technique [17], i.e. it introduces minimal damage to the least depth material. Our data prove that EDM cutting is not recommended *after* shot peening treatment – we believe that the re-distribution/relaxation of residual stresses may cause very detrimental effect.

Preprints (www.preprints.org) | NOT PEER-REVIEWED | Posted: 4 March 2022 doi:10.20944/preprints202203.0080.v1

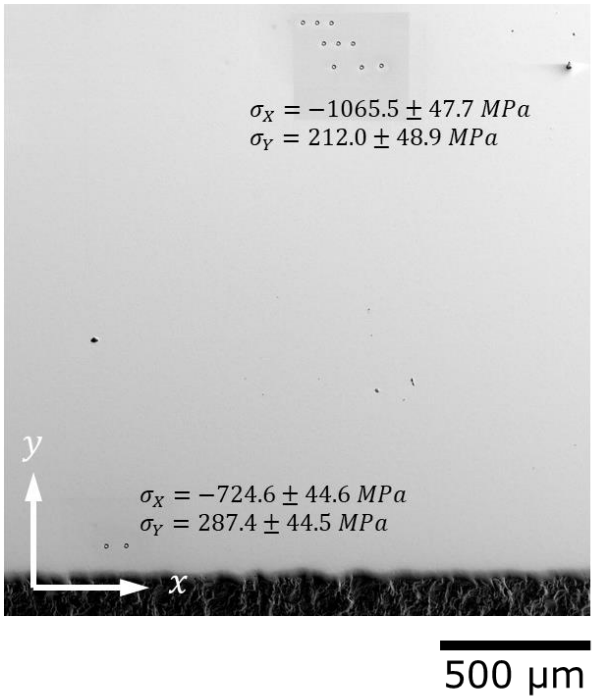


**Figure 9.** RS under shot peened area - ***Face III*** 7.5x5 mm$^2$

***Face III*** is parallel to the shot peened surface and lays at the depth of about 80 µm. As one can see accurate preparation of the sample for EBSD studies fully eliminates surface scratches as well as all signs of shot peening. The sequence of polishing operations does redistribute residual stresses present before polishing and introduce new residual stresses, on the other hand, we believe that polishing techniques applied [18] are much less intensive than shot peening and no substitutional changes are caused by polishing as it is. The redistribution and relaxation of residual stresses due to the elimination of stressed surface layers seem to be predominantly responsible for the appearance of tensile in-plane residual stresses. The contribution of out-of-plane (which are discussed below) is suspected to introduce harmful tensile stresses, which may facilitate surface cracks nucleation and growth. Therefore, polishing is also not recommended *after* shot peening treatment.

*Profiling of residual stresses in depth.* Figure 10a shows the locations of probing FIB core-ring holes – different ring diameters, distances and number of repetitions were applied in order to reach satisfactory spatial resolution and statistical fidelity within sub-surface layers and to optimize ion drilling time and Ga-consumptions. Sub-surface $\sigma_y$ stress profile (in-plane stresses, parallel to shot peened surface) starts from the depth of 40 µm with the value of -600 MPa. The estimation for the same orientation of residual stresses at the surface is -500 MPa and it perfectly agrees with the expected decrease towards deeper layers.

Preprints (www.preprints.org) | NOT PEER-REVIEWED | Posted: 4 March 2022 doi:10.20944/preprints202203.0080.v1

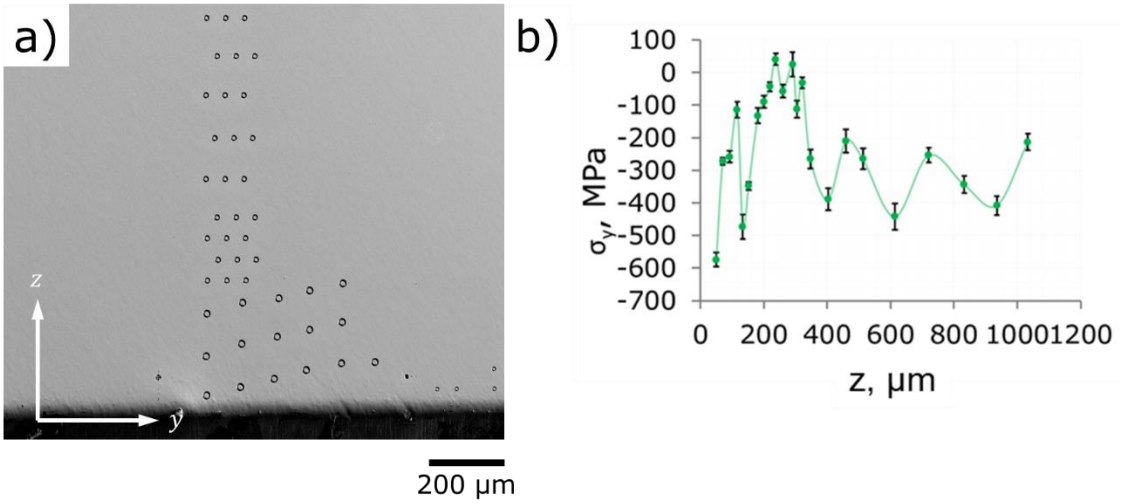


**Figure 10.** Depth distribution of RS in shot peened area - the middle of sample - a) SEM image of probing FIB core-ring holes at ***Face I*** 7.5x3 mm$^2$; b) profiles of $\sigma_y$ and $\sigma_z$ against depth

In contrast to anticipated RS profile, maximum that is reached at the distance of about 300 µm from the surface gives near-zero values, while the steady level of RS that starts at the distance of 400 µm from the surface corresponds to compression zone with stable residual stresses in the range -400…200 MPa.

Sub-surface $\sigma_z$ stress profile (out-of-plane stresses, perpendicular to shot peened surface) is asymmetrical to the $\sigma_y$ stress profile - modest tensile stresses at shallow depth, minimum stresses at the depth of about 300 µm from the surface (about -400 MPa) and stabilization at near-zero stress values at the depth of about 400 µm from the surface. Out-of-plane stresses cannot be measured using X-ray diffraction ($sin^2\psi$) or hole drilling methods and they are commonly considered as null at the surface from static mechanics point of view. FIB core-ring method, nevertheless, detects significant (+300 MPa) tensile stresses in sub-surface layer at the depth of 40 µm. This fact should not be neglected since the same phenomenon is reproducible at ***Face II*** as demonstrated in Figure 11.

Preprints (www.preprints.org) | NOT PEER-REVIEWED | Posted: 4 March 2022 doi:10.20944/preprints202203.0080.v1

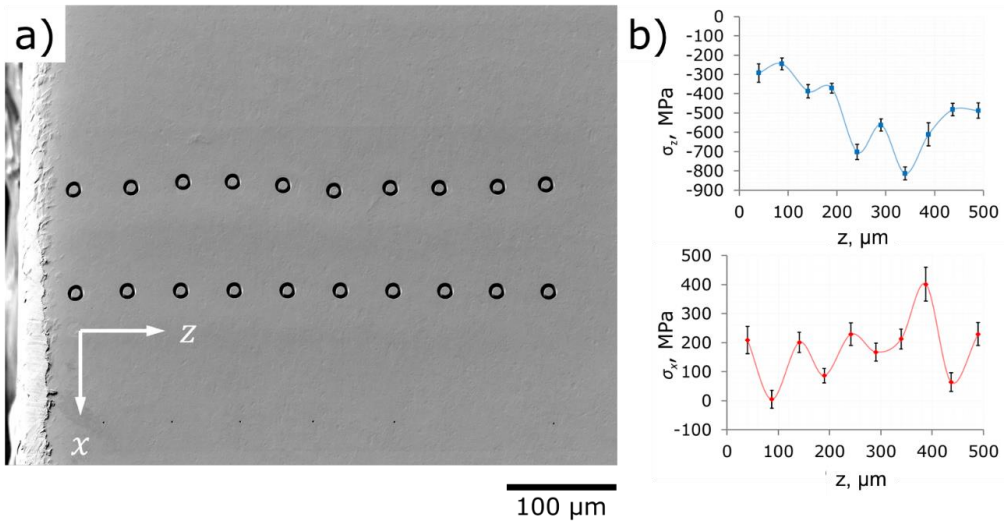


**Figure 11.** Depth distribution of RS in shot peened area - the edge of sample - a) SEM image of probing FIB core-ring holes at ***Face II*** 5x3 mm$^2$; b) profiles of $\sigma_x$ and $\sigma_z$ against depth

Sub-surface $\sigma_x$ stress profile (in-plane stresses, parallel to shot peened surface) build at the sample edge is dramatically different from that in the middle of shot peened area suggesting specific conditions of shot peening treatment at the edge. No maximum of residual stresses at the depth of about 300 µm was found, in contrast, a minimum (-800 MPa) was discovered. In general, ***Face II*** shows relatively strong (-800…-200 MPa) compressive residual stresses at the distances 40…500 µm from the surface. This also corresponds to the estimations for surface in-plane residual stresses obtained at the sample edge (location 12 in Figure 8a).

Out-of-plane residual stresses $\sigma_z$ are nill at the shallowest depth and then raise with the distance from the surface to the values in the range of 100…400 MPa with no distinct tendency. The origin of these stresses is not fully clear and they can be thought as the relicts of previous treatments, e.g. plate rolling.

## 4 Conclusions

FIB core-ring drilling technique of residual stress evaluation exists as approved for about 15 years and nowadays it becomes possible to correlate and compare the measurements conducted at dramatically different dimensional scales - from units of micrometers to units of millimeters. Methodological issues of representativity of microscopic volumes for measurements of Type I residual stresses and averaging of residual stresses over grain assemblies need to be answered for scientific and practical uses.

We selected a well-studied subject - shot peening treatment for the introduction of compressive residual stresses into surface layers of parts susceptible to fatigue - for comparative case study and applied

macroscopic destructive and non-destructive (hole drilling and X-ray diffraction) and microscopic (FIB core-ring drilling) methods.

We conclude that thin and slim samples after shot peening are hardly to be adequately studied with hole drilling method when few mm big drills are used - thin subsurface layers seems to be held out of relaxation by core layers of material.

X-ray diffraction is in good agreement with FIB core-ring drilling - both methods return high values of compressive residual stresses of about -500 MPa.

FIB core-ring method is a favorable method of residual stress evaluation when fine details (as well as thin and slim samples or small cross-sections) of residual stress spatial distribution or depth profiles are wanted to be characterized. We prove that this method fairly agrees with X-rays diffraction method (own data) and hole drilling method (literature data) in terms of signs, values and depth profiles. It also allows detecting of relaxation and stress redistribution effects close to the geometrical or physical peculiarities of a sample - edges, cuts and transition zones.

Out-of-plane residual stresses found in the shallow sub-surface layers evoke significant interest since they are, being tensile, may promote delamination cracks, which are only seemingly less harmful, but may reduce efficient cross-section and redistribute useful residual stresses.

## CRediT authorship contribution statement

**Somov P.A.**: Data curation, Methodology. **Statnik E.S.**: Writing – review & editing, Data curation, Formal analysis, Conceptualization, Visualization. **Kan Yu.**: Data curation, Methodology, Writing – review & editing. **Pisarev V.S.**: Data curation, Methodology. **Eleonsky S.I.**: Data curation, Methodology. **Ozherelkov D.Yu.**: Resources, Data curation. **Salimon A.I.**: Writing – original draft, Supervision, Project administration, Funding acquisition.

## Declaration of Competing Interest

The authors declare that they have no known competing financial interests or personal relationships that could have appeared to influence the work reported in this paper.

## Funding

This research was funded by the Russian Science Foundation, grant number 21-19-00791, https://rscf.ru/en/project/21-19-00791/.

**Acknowledgments**

This research was funded by the Russian Science Foundation, grant number 21-19-00791, https://rscf.ru/en/project/21-19-00791/. The authors are grateful to the crew of Fablab (Skoltech, Moscow, Russia) for their delicate and accurate sample preparations.

**References**

1 Mugwagwa L., Yadroitsava I., Makoana N.W., Yadroitsev I. Residual stress in laser powder bed fusion. Fundamentals of Laser Powder Bed Fusion of Metals, *Additive Manufacturing Materials and Technologies* **2021**, 245-276.

2 Manchoul S., Sghaier R.B., Seddik R. and Fathallah R. Comparison between conventional shot peening and ultrasonic shot peening. *Mechanics & Industry* **2018**, 19, 6.

3 Korsunsky A.M. The modelling of residual stresses due to surface peening using eigenstrain distributions. *J. Strain Analysis* **2005**, 40, 8, 817-824.

4 Bagherifard S., Guagliano M. Review of shot peening processes to obtain nanocrystalline surfaces in metal alloys. *Surface Engineering* **2009**, 25, 1, 3-14.

5 Winiarski B., Benedetti M., Fontanari V. *et al.* High Spatial Resolution Evaluation of Residual Stresses in Shot Peened Specimens Containing Sharp and Blunt Notches by Micro-hole Drilling, Micro-slot Cutting and Micro-X-ray Diffraction Methods. *Exp Mech* **2016**, 56, 1449-1463.

6 Salvati E., Benedetti M., Sui T., Korsunsky A.M. Residual Stress Measurement on Shot Peened Samples Using FIB-DIC. *Conference of SEM* **2015**, Costa Mesa - California.

7 Everaerts J., Song X., Nagarajan B., Korsunsky A.M. Evaluation of macro- and microscopic residual stresses in laser shock-peened titanium alloy by FIB-DIC ring-core milling with different core diameters. *Surface and Coatings Technology* **2018**, 349, 719-724.

8 Korsunsky A.M., Sebastiani M., Bemporad E. Focused ion beam ring drilling for residual stress evaluation. *Materials Letters* **2009**, 63, 22, 1961-1963.

9 Schajer G.S. Advances in hole-drilling residual stress measurement. *Exp. Mech.* **2010**, 50, 159-168.

10 V.S. Pisarev, I.N. Odintsev, S.I. Eleonsky, A.A. Apalkov. Residual stress determination by optical interferometric measurements of hole diameter increments. *Opt. and Las. in Eng.* **2018**, 110, 437-456.

11 V.S. Pisarev, S.I. Eleonsky, A.V. Chernov, Residual stress determination in orthotropic composites by displacement measurements near through hole. *Exp. Mech.* **2015**, 55, 1225-1238.

12 Oliver W.C., Pharr G.M. An improved technique for determining hardness and elastic modulus using load and displacement sensing indentation experiments. *J. Mater. Res.* **1992**, 7, 1564-1583.

13 Yetna N'Jocka M., Roudet F.; Idriss M.; Bartier O.; Chicot D. Work-of-indentation coupled to contact stiffness for calculating elastic modulus by instrumented indentation. *Mech. Mater.* **2016**, 94, 170-179.

14 Lord Jerry, Cox David, Ratzke Agnieszka, Sebastiani Marco, Korsunsky Alexander, Mughal Muhammad, Salvati Enrico. A Good Practice Guide for Measuring Residual Stresses using FIB-DIC. *National Physical Laboratory (Teddington, UK)* **2018**.

15 Melanie Senn. Digital Image Correlation and Tracking (https://www.mathworks.com/matlabcentral/fileexchange/50994-digital-image-correlation-and-tracking), *MATLAB Central File Exchange*. Retrieved November 30, **2021**.

16 Korsunsky A.M. A critical discussion of the $sin^2\psi$ stress measurement technique. *Materials Science Forum* **2008**, 571, 219-224.

17 Uzun F., Everaerts J., Brandt L.R., Kartal M., Salvati E., Korsunsky A.M. The inclusion of short-transverse displacements in the eigenstrain reconstruction of residual stress and distortion in in740h weldments. *Journal of Manufacturing Processes* **2018**, 36, 601-612.

18 Gurova T., Teodosio J.R., Rebello J.M.A., Monin V. Model for the variation of the residual stress state during plastic deformation under uniaxial tension. *The Journal of Strain Analysis for Engineering Design* **1998**, 33(5), 367-372.